



ISSN 1001-0742

CN 11-2629/X

2012

Volume **24**
Number **7**

JOURNAL OF
**ENVIRONMENTAL
SCIENCES**



Sponsored by
Research Center for Eco-Environmental Sciences
Chinese Academy of Sciences

JOURNAL OF ENVIRONMENTAL SCIENCES

(<http://www.jesc.ac.cn>)

Aims and scope

Journal of Environmental Sciences is an international academic journal supervised by Research Center for Eco-Environmental Sciences, Chinese Academy of Sciences. The journal publishes original, peer-reviewed innovative research and valuable findings in environmental sciences. The types of articles published are research article, critical review, rapid communications, and special issues.

The scope of the journal embraces the treatment processes for natural groundwater, municipal, agricultural and industrial water and wastewaters; physical and chemical methods for limitation of pollutants emission into the atmospheric environment; chemical and biological and phytoremediation of contaminated soil; fate and transport of pollutants in environments; toxicological effects of terrorist chemical release on the natural environment and human health; development of environmental catalysts and materials.

For subscription to electronic edition

Elsevier is responsible for subscription of the journal. Please subscribe to the journal via <http://www.elsevier.com/locate/jes>.

For subscription to print edition

China: Please contact the customer service, Science Press, 16 Donghuangchenggen North Street, Beijing 100717, China. Tel: +86-10-64017032; E-mail: journal@mail.sciencep.com, or the local post office throughout China (domestic postcode: 2-580).

Outside China: Please order the journal from the Elsevier Customer Service Department at the Regional Sales Office nearest you.

Submission declaration

Submission of an article implies that the work described has not been published previously (except in the form of an abstract or as part of a published lecture or academic thesis), that it is not under consideration for publication elsewhere. The submission should be approved by all authors and tacitly or explicitly by the responsible authorities where the work was carried out. If the manuscript accepted, it will not be published elsewhere in the same form, in English or in any other language, including electronically without the written consent of the copyright-holder.

Submission declaration

Submission of the work described has not been published previously (except in the form of an abstract or as part of a published lecture or academic thesis), that it is not under consideration for publication elsewhere. The publication should be approved by all authors and tacitly or explicitly by the responsible authorities where the work was carried out. If the manuscript accepted, it will not be published elsewhere in the same form, in English or in any other language, including electronically without the written consent of the copyright-holder.

Editorial

Authors should submit manuscript online at <http://www.jesc.ac.cn>. In case of queries, please contact editorial office, Tel: +86-10-62920553, E-mail: jesc@263.net, jesc@rcees.ac.cn. Instruction to authors is available at <http://www.jesc.ac.cn>.

Copyright

© Research Center for Eco-Environmental Sciences, Chinese Academy of Sciences. Published by Elsevier B.V. and Science Press. All rights reserved.

CONTENTS

Aquatic environment

Investigation of the hydrodynamic behavior of diatom aggregates using particle image velocimetry Feng Xiao, Xiaoyan Li, Kitming Lam, Dongsheng Wang.....	1157
Shellac-coated iron oxide nanoparticles for removal of cadmium(II) ions from aqueous solution Jilai Gong, Long Chen, Guangming Zeng, Fei Long, Jiuhua Deng, Qiuya Niu, Xun He.....	1165
Prediction of DOM removal of low specific UV absorbance surface waters using HPSEC combined with peak fitting Linan Xing, Rolando Fabris, Christopher W. K. Chow, John van Leeuwen, Mary Drikas, Dongsheng Wang.....	1174
Photo-production of dissolved inorganic carbon from dissolved organic matter in contrasting coastal waters in the southwestern Taiwan Strait, China Weidong Guo, Liyang Yang, Xiangxiang Yu, Weidong Zhai, Huasheng Hong.....	1181
One century sedimentary record of lead and zinc pollution in Yangzong Lake, a highland lake in southwestern China Enlou Zhang, Enfeng Liu, Ji Shen, Yanmin Cao, Yanling Li.....	1189
Antimony(V) removal from water by iron-zirconium bimetal oxide: Performance and mechanism Xuehua Li, Xiaomin Dou, Junqing Li.....	1197
Carbonaceous and nitrogenous disinfection by-product formation in the surface and ground water treatment plants using Yellow River as water source Yukun Hou, Wenhai Chu, Meng Ma.....	1204
Water quality evaluation based on improved fuzzy matter-element method Dongjun Liu, Zhihong Zou.....	1210
Formation and cytotoxicity of a new disinfection by-product (DBP) phenazine by chloramination of water containing diphenylamine Wenjun Zhou, Linjie Lou, Lifang Zhu, Zhimin Li, Lizhong Zhu.....	1217

Atmospheric environment

Chemical compositions of PM _{2.5} aerosol during haze periods in the mountainous city of Yong'an, China Liqian Yin, Zhenchuan Niu, Xiaoqiu Chen, Jinsheng Chen, Lingling Xu, Fuwang Zhang.....	1225
Decomposition of trifluoromethane in a dielectric barrier discharge non-thermal plasma reactor M. Sanjeeva Gandhi, Y. S. Mok.....	1234
Transverse approach between real world concentrations of SO ₂ , NO ₂ , BTEX, aldehyde emissions and corrosion in the Grand Mare tunnel I. Ameur-Bouddabbous, J. Kasperek, A. Barbier, F. Harel, B. Hannoyer.....	1240
A land use regression model incorporating data on industrial point source pollution Li Chen, Yuming Wang, Peiwu Li, Yaqin Ji, Shaofei Kong, Zhiyong Li, Zhipeng Bai.....	1251

Terrestrial environment

Effect of vegetation of transgenic Bt rice lines and their straw amendment on soil enzymes, respiration, functional diversity and community structure of soil microorganisms under field conditions Hua Fang, Bin Dong, Hu Yan, Feifan Tang, Baichuan Wang, Yunlong Yu.....	1259
Enhanced flushing of polychlorinated biphenyls contaminated sands using surfactant foam: Effect of partition coefficient and sweep efficiency Hao Wang, Jiajun Chen.....	1270
Transpiration rates of urban trees, <i>Aesculus chinensis</i> Hua Wang, Xiaoke Wang, Ping Zhao, Hua Zheng, Yufen Ren, Fuyuan Gao, Zhiyun Ouyang.....	1278

Environmental biology

Methanogenic community dynamics in anaerobic co-digestion of fruit and vegetable waste and food waste Jia Lin, Jiane Zuo, Ruofan Ji, Xiaojie Chen, Fenglin Liu, Kaijun Wang, Yunfeng Yang.....	1288
Differential fate of metabolism of a disperse dye by microorganisms <i>Galactomyces geotrichum</i> and <i>Brevibacillus laterosporus</i> and their consortium GG-BL Tatoba R. Waghmode, Mayur B. Kurade, Anuradha N. Kagalkar, Sanjay P. Govindwar.....	1295

Environmental catalysis and materials

Effects of WO _x modification on the activity, adsorption and redox properties of CeO ₂ catalyst for NO _x reduction with ammonia Ziran Ma, Duan Weng, Xiaodong Wu, Zhichun Si.....	1305
Photocatalytic degradation of bisphenol A using an integrated system of a new gas-liquid-solid circulating fluidized bed reactor and micrometer Gd-doped TiO ₂ particles Zhiliang Cheng, Xuejun Quan, Jinxin Xiang, Yuming Huang, Yunlan Xu.....	1317
Effect of CeO ₂ and Al ₂ O ₃ on the activity of Pd/Co ₃ O ₄ /cordierite catalyst in the three-way catalysis reactions (CO/NO/C _n H _m) Sergiy O. Soloviev, Pavlo I. Kyriienko, Nataliia O. Popovych.....	1327

Environmental analytical methods

Development of indirect competitive fluorescence immunoassay for 2,2',4,4'-tetrabromodiphenyl ether using DNA/dye conjugate as antibody multiple labels Zi-Yan Fan, Young Soo Keum, Qing-Xiao Li, Weilin L. Shelver, Liang-Hong Guo.....	1334
A novel colorimetric method for field arsenic speciation analysis Shan Hu, Jinsuo Lu, Chuanyong Jing.....	1341
Aminobenzenesulfonamide functionalized SBA-15 nanoporous molecular sieve: A new and promising adsorbent for preconcentration of lead and copper ions Leila Hajiaghatabaei, Babak Ghasemi, Alireza Badieli, Hassan Goldoos, Mohammad Reza Ganjali, Ghodsi Mohammadi Ziarani.....	1347



A land use regression model incorporating data on industrial point source pollution

Li Chen^{1,*}, Yuming Wang¹, Peiwu Li¹, Yaqin Ji^{2,3,*}, Shaofei Kong^{2,3}, Zhiyong Li^{2,3}, Zhipeng Bai⁴

1. College of Urban and Environmental Science, Tianjin normal University, Tianjin 300387, China

2. College of Environmental Science and Engineering, Nankai University, Tianjin 300071, China

3. State Environmental Protection Key Laboratory of Urban Ambient Air Particulate Matter Pollution and Control, Tianjin 300071, China

4. Chinese Research Academy of Environmental Sciences, Beijing 100012, China

Received 20 August 2011; revised 3 February 2012; accepted 25 February 2012

Abstract

Advancing the understanding of the spatial aspects of air pollution in the city regional environment is an area where improved methods can be of great benefit to exposure assessment and policy support. We created land use regression (LUR) models for SO₂, NO₂ and PM₁₀ for Tianjin, China. Traffic volumes, road networks, land use data, population density, meteorological conditions, physical conditions and satellite-derived greenness, brightness and wetness were used for predicting SO₂, NO₂ and PM₁₀ concentrations. We incorporated data on industrial point sources to improve LUR model performance. In order to consider the impact of different sources, we calculated the PSIndex, LSIndex and area of different land use types (agricultural land, industrial land, commercial land, residential land, green space and water area) within different buffer radii (1 to 20 km). This method makes up for the lack of consideration of source impact based on the LUR model. Remote sensing-derived variables were significantly correlated with gaseous pollutant concentrations such as SO₂ and NO₂. R² values of the multiple linear regression equations for SO₂, NO₂ and PM₁₀ were 0.78, 0.89 and 0.84, respectively, and the RMSE values were 0.32, 0.18 and 0.21, respectively. Model predictions at validation monitoring sites went well with predictions generally within 15% of measured values. Compared to the relationship between dependent variables and simple variables (such as traffic variables or meteorological condition variables), the relationship between dependent variables and integrated variables was more consistent with a linear relationship. Such integration has a discernable influence on both the overall model prediction and health effects assessment on the spatial distribution of air pollution in the city region.

Key words: land use regression; air pollution; Tianjin; point source; GIS

DOI: 10.1016/S1001-0742(11)60902-9

Introduction

The capacity to accurately assess personal exposures to air pollution is important for epidemiological studies on the health effects of air pollution (Slama et al., 2007). When the effects of intra-urban differences in exposure are studied, the use of monitoring sites is likely to be inadequate for representing the spatial variability that exists within a city region.

Land use regression (LUR) is used to model the concentrations of air pollutants as a function of the most predictive variables (traffic, land use, population, meteorological conditions and physical conditions), and GIS is used to render the models as maps that can estimate exposure across the study area (Briggs et al., 1997; Briggs et al., 2005; Gilbert et al., 2005; Jerrett et al., 2005; Ross et al., 2007; Kashima et al., 2009; Beelen et al., 2009; Mukerjee et al., 2009). Several recent studies demonstrated the potential of LUR to supply accurate, small-area estimates of dispersion or

exposure modeling (Briggs et al., 2000; Brauer et al., 2003; Henderson et al., 2007; Hoek et al., 2008; Mavko et al., 2008). Furthermore, some other studies have considered the impact of meteorological conditions and physical conditions while predicting air pollutant concentrations (Arain et al., 2007; Su et al., 2007; Mavko et al., 2008; Ryan et al., 2008). Area sources and line sources can be represented by land use variables and traffic variables, respectively. But the impact of point sources has not been fully considered.

This article reports the first attempt to model SO₂, NO₂ and PM₁₀ concentrations in Tianjin using a LUR approach. The aim of our study was to assess the extension of the application as well as the accuracy improvement of LUR. Three tasks were conducted: (1) to reveal whether or not the LUR model performance will be improved when the impact of point sources is considered; (2) to examine the LUR model performance considering the underlying surface conditions of monitoring sites based on remote sensing data; (3) to establish multiple linear regression equations using integrated independent variables (such as LSIndex).

* Corresponding author. E-mail: amychenli1981@126.com (Li Chen); jiyaqin@nankai.edu.cn (Yaqin Ji)

1 Methods

1.1 Study area

Tianjin, located about 120 km southeast of Beijing, is the largest coastal city in northern China with a total population of over 10 million and an area of 11,920 km² (Fig. 1). There are 15 districts and 3 counties in Tianjin. In general, the 18 administrative districts range from very urban to relatively rural. The population distribution among the 18 districts is as follows: 10 districts have fewer than 0.5 million people each (with a minimum population of 0.17 million in Hangu District), while 2 districts have a population of more than 0.8 million (with a maximum population of 0.82 million in Wuqing District). The average annual temperature and annual precipitation are 12.3°C and 550–680 mm, respectively. As an industrial city, the major industries in Tianjin include electronics, automobile, petrochemical, metallurgy, biomedical, new energy, etc. By the end of 2006, there were 1.196 million automobiles in Tianjin. The number of private cars has been growing at a rate of nearly 20% every year since 2004. The increasing fuel consumption, number of construction projects, and continuous population expansion have brought serious air pollution problems to the city, where PM₁₀ has been observed as the principal air pollutant. The

number of days when PM₁₀ was the principal air pollutant accounted for 80% (305 days) of the year of 2006.

1.2 Dependent variables of ambient SO₂, NO₂ and PM₁₀ monitoring data

The purpose for establishing a regional environmental air monitoring network is to confirm the possibly high levels of air pollutants, the influence of the most important sources of air pollution on environmental air quality, the background level of air pollutants, and the variation trends for air pollutants, and to provide support for the constitution of a local air pollution control layout. The monitoring sites were representative of areas with greater population density, a variety of land use types and high traffic areas.

SO₂ (API-110, ultraviolet fluorescence), NO₂ (Thermal instruments, Anhui Landun Phototelectron Co., Ltd., China), and PM₁₀ (RP1400 based on TEOM method) monitoring data from regulatory sites operated and managed by the Tianjin Institute of Environmental Sciences were used (Tianjin Bureau of Environmental Protection, 2007). QA/QC procedures at each monitoring site were followed according to the Automated Methods for Ambient Air Quality Monitoring issued by the Ministry of Environmental Protection. SO₂ and NO₂ concentrations were recorded every minute, and the PM₁₀ concentration was recorded every hour. The automated monitoring instrument took samples all day (24 hr). The SO₂, NO₂ and PM₁₀ concentrations were recorded for a whole year.

1.3 Independent variables

In this study, the candidate independent variables included traffic variables (length of the major roads, traffic volume and distance to expressway), land use variables (areas of agricultural land, industrial land, commercial land, residential land, green space and water area within different buffer radii), population density, meteorological variables (wind frequency, wind speed, temperature and relative humidity), physical variables (brightness, greenness, wetness, distance to sea and elevation), and pollution source variables (point source, line source and area source). The relationships between a dependent variable and each independent variable were simulated, but they were not all linear. Some independent variables (such as the pollution source variables and meteorological variables) were integrated, so as to be more consistent with a linear relationship between the integrated independent variable (such as LSIndex) and dependent variable.

1.4 Tasseled Cap Transformation

The Tasseled Cap Transformation in remote sensing is the conversion of the readings in a set of channels into composite values; i.e., the weighted sums of separate channel readings. One of these weighted sums measures roughly the brightness of each pixel in the scene. The other composite values are linear combinations of the values of the separate channels, but some of the weights are negative and others positive. One of these other composite values represents the degree of greenness of the pixels and another

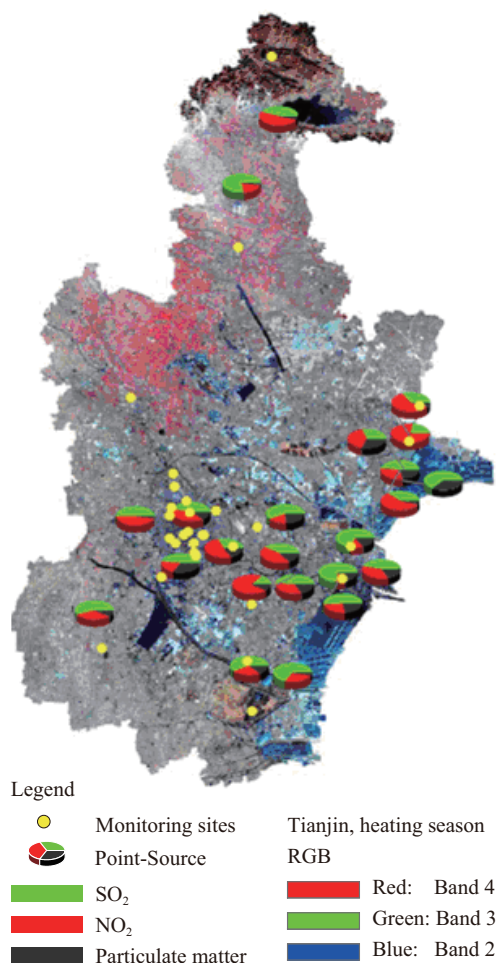


Fig. 1 Study area location, monitoring sites and point sources. Landsat TM color image composition scheme of bands 4, 3, 2.

represents the degree of wetness of the soil. Usually there are just three composite variables (Crist and Cicone, 1984). The weights for Tasseled Cap Transformation of Thematic Mapper data were 0.3037, 0.2793, 0.4343, 0.5585, 0.5082 and 0.1863 (for Brightness); -0.2848 , -0.2435 , -0.5436 , 0.7243 , 0.0840 and -0.1800 (for Greenness); and 0.1509 , 0.1793 , 0.3299 , 0.3406 , -0.7112 and -0.4572 (for Wetness) for Channel 1, 2, 3, 4, 5 and 7, respectively (Crist and Cicone, 1984). Because of the complexities involved in the display and extraction of information contained in the Landsat TM data, the tasseled-cap transformation was used to reduce the number of channels to be considered, and to provide a more direct association between signal response and underlying surface conditions (Crist and Cicone, 1984).

Tasseled-cap indices for Tianjin were derived from the TM data collected from a nominal altitude of 705 km in a near-polar, near-circular, sun-synchronous orbit. The imagery we acquired included three visible (resolution 30 m), three infrared (30 m), and one thermal (120 m) band. The scenes for Tianjin were captured on December 28 and July 21, 2006. These images were projected to Universal Transverse Mercator (UTM) with a WGS84 datum. The brightness, greenness and wetness of each monitoring site were calculated based on ENVI 4.5. Because the dependent variables were the annual average SO_2 , NO_2 and PM_{10} concentrations, two remote sensing images were used (December 28 and July 21, 2006), and the brightness, greenness and wetness average values were calculated based on the two images.

1.5 Point source variable

There were 17 thermal power plants and 6 coal-fired plants that were considered in the study area. To account for the location of the monitoring site relative to the wind direction and the distance from monitoring site to point source, the PSIndex was calculated. The point sources included thermal power plants and coal-fired plants.

$$\text{PSIndex} = \sum_{i=1}^n \frac{RA_i W_{ij}}{D_{ij}} \quad (1)$$

where, i is the ID of the point source; j is the ID of the monitoring site; n is the number of the point source in the buffer within R for the j th monitoring site; R (km) is the buffer radius; D_{ij} (km) is the distance from the j th monitoring site to the i th point source; A_i (ton) is the amount of air pollutants (particulate matter, SO_2 and NO_2) of the i th point source in 2006; W_{ij} (%) is the wind frequency of the j th monitoring site from the i th point source; and PSIndex is the point source index. The data for A_i were obtained from the Tianjin environmental quality report (Tianjin Bureau of Environmental Protection, 2007).

1.6 Line source variable

There were 174 roads that were considered in this study. To account for the location of each monitoring site relative to the wind direction and the distance from the monitoring

site to line source, the LSIndex was calculated.

$$\text{LSIndex} = \sum_{i=1}^n \frac{c_i R L_i W_{ij}}{D_{ij}} \quad (2)$$

where, i is the ID of the line source; j is the ID of the monitoring site; n is the number of the line source in the buffer within R ; R (km) is the buffer radius; D_{ij} (km) is the distance from the j th monitoring site to the i th line source; L_i (km) is the length of the i th road in the buffer within R ; W_{ij} (%) is the wind frequency of the j th monitoring site from the i th point source; c_i is the class index of the i th line source, and LSIndex is the line source index.

Five types of roadway configuration and traffic volume data were analyzed for their ability to predict traffic-related pollution, and the class index was calculated based on the traffic volume (Table 1).

Table 1 Road classification hierarchy

Road classification	Traffic volume (vehicles/day)	Class index (c)
Express way	7000–25000	0.320
First Class road	4500–7000	0.115
Second Class road	2000–4500	0.065
Third Class road	200–2000	0.022
Fourth Class road	0–200	0.002

“ c ” was calculated based on the weight of traffic volume of its road classification.

1.7 Area source variable

Most land use variables in LUR models applied to data were originally derived from remote sensing data. The most comprehensive, high-resolution remote sensing data (six bands finer than 30 m and one band 120 m) are Landsat Thematic Mapper (TM) data. Using Landsat TM data, the land use types were classified into agricultural land, industrial land, commercial land, residential land, green space and water area based on ENVI4.5. The classification method was supervised classification, and field investigation was used to verify the result of the classification. The classification results were as follows: the total accuracy of the class accuracy evaluation was 0.906 and the Kappa coefficient was 0.885.

2 Results

2.1 Descriptive statistics for air pollutants

The annual average concentrations for SO_2 , NO_2 and PM_{10} were approximately normally distributed with a mean for SO_2 of 0.064 mg/m^3 (range: $0.034\text{--}0.084 \text{ mg/m}^3$; SD = 0.012), for NO_2 of 0.047 mg/m^3 (range: $0.026\text{--}0.066 \text{ mg/m}^3$; SD = 0.011) and for PM_{10} of 0.111 mg/m^3 (range: $0.094\text{--}0.132 \text{ mg/m}^3$; SD = 0.008) (Fig. 2). All statistics above were based on the full set of samples with no validation samples removed.

2.2 Point source variable at Tanggu monitoring site

To observe a decrease in the influence of certain emission sources after a large enough distance, the PSIndex

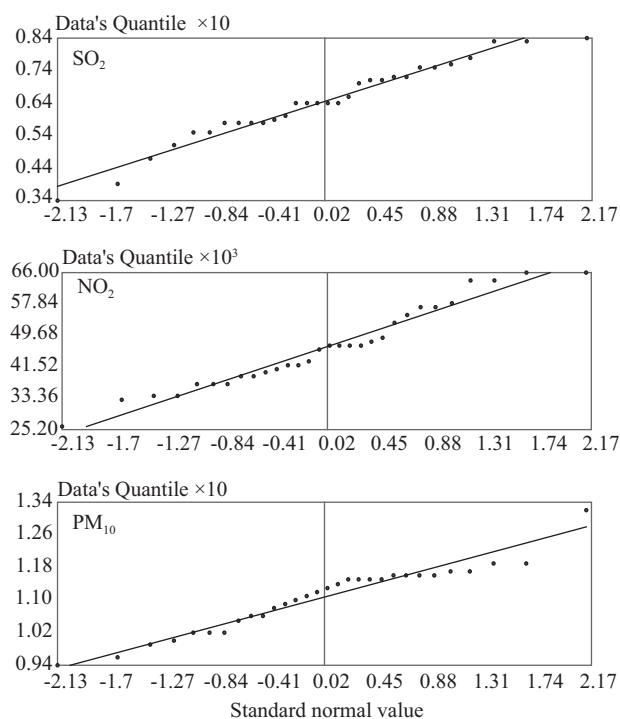


Fig. 2 Normal QQ plots of the measured air pollutants concentrations. In general, the points lie close to the straight line, which indicates perfect normality. The main departure from this line occurs at high or low values.

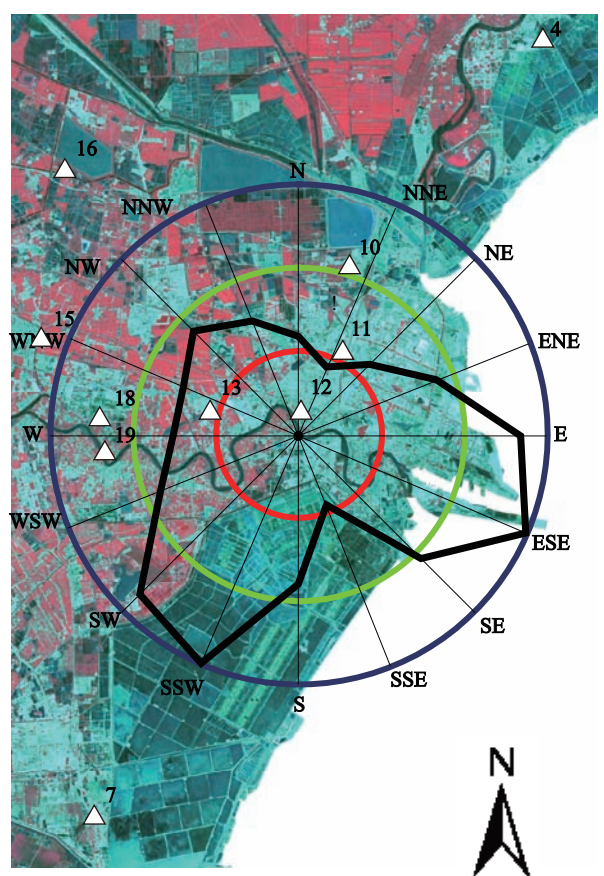
was calculated based on different R values (1 to 20 km), and the Pearson Correlation was calculated between PSIndex-SO₂ and SO₂ concentration, PSIndex-NO₂ and NO₂ concentration, and PSIndex-PM₁₀ and PM₁₀ concentration, respectively. The appropriate PSIndex- R was 15 km based on the Pearson Correlation. Figure 3 shows the location of the Tanggu monitoring site, point sources within 15 km around the Tanggu monitoring site and the wind frequency of the Tanggu monitoring site in 2006. Table 2 shows the point source parameters at the Tanggu monitoring site, and the PSIndex-SO₂, -NO₂ and -PM₁₀ for the Tanggu monitoring site were 211283.60, 114801.10 and 92781.23, respectively, based on Eq. (1). Then, the PSIndex of each monitoring site was calculated in this way.

2.3 Line source variable at Tanggu monitoring site

The LSIndex was calculated based on different R values (1 to 20 km), and the Pearson Correlation was calculated between the LSIndex and the SO₂, NO₂ and PM₁₀ concentrations, respectively. The appropriate LSIndex- R was 5 km based on the Pearson Correlation. Figure 4 shows the location of the Tanggu monitoring site, line sources within 5 km around the Tanggu monitoring site and wind frequency of the Tanggu monitoring site in 2006. Table 3

Table 2 Point-source variable parameter at the Tanggu monitoring site

Point-source ID	12	11	13	10	18	19
D (km)	1.75	5.69	5.55	10.44	11.77	11.81
$A_{PM_{10}}$ (ton)	1132.20	1368.80	620.70	2480	52.20	1477.70
A_{SO_2} (ton)	2551.20	3871.20	2750.00	1127.20	84.40	4250.00
A_{NO_2} (ton)	1318.60	3059.60	413.00	257.20	474.80	2961.80
W (%)	4.00	5.00	5.00	5.00	5.00	5.00



Legend

- Monitoring sites
- △ Point-source
- Buffer within 5 km
- Buffer within 10 km
- Buffer within 15 km
- wind rose

Fig. 3 Point sources within 5, 10 and 15 km buffer radii and wind rose at the Tanggu monitoring site in 2006.

shows the line source parameters at the Tanggu monitoring site, and the LSIndex was 19.27 based on Eq. (2). Then, the LSIndex of each monitoring site was calculated in the same way.

2.4 Regression model building and results

Independent variables with univariate associations significant at $p \leq 0.05$ were considered for multivariate models for LUR equations. Remote sensing-derived brightness and greenness were correlated highly with SO₂ (correlation coefficient = 0.55) and NO₂ concentrations (correlation coefficient = 0.63). The brightness, greenness and wetness images, shown in Fig. 5a, b, c, demonstrated the underlying surface conditions of monitoring sites.

Table 3 Line-source variable parameters at the Tanggu monitoring site

Road number	1	2	3	4	5	6
D (km)	2440.74	3657.47	3705.89	2809.42	926.19	3943.13
L (km)	6432.37	4309.26	1951.37	6049.18	6318.16	6870.43
c	0.115	0.115	0.115	0.022	0.022	0.022
W (%)	3	10	6	6	5	5

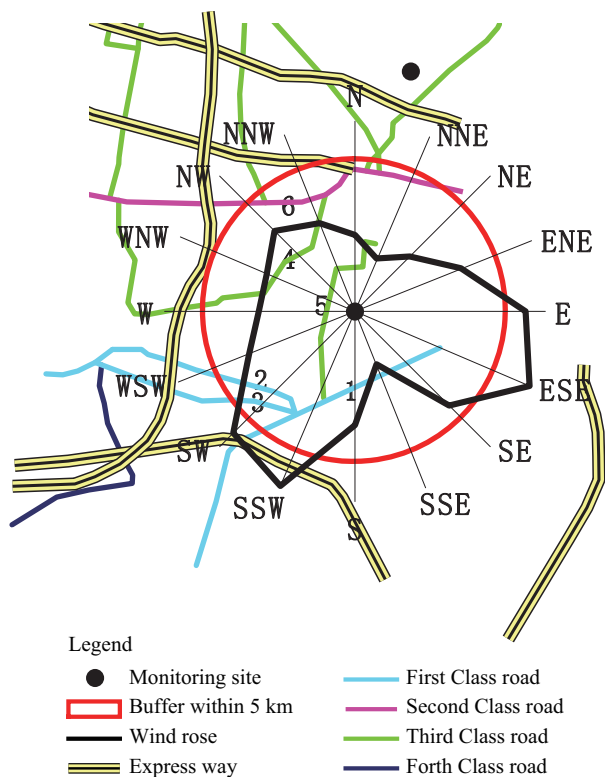


Fig. 4 Roads (five levels) within 5 km buffer radius and wind rose at the Tangu monitoring site in 2006. 1–6 mean road number.

The independent variables for the LUR (SO_2) model included PSIndex- SO_2 , LSIndex, area of residential land within 2 km buffer radius and brightness. The independent variables for the LUR (NO_2) model included PSIndex- NO_2 , LSIndex, distance to expressway and greenness. The independent variables for the LUR (PM_{10}) model included population density, PSIndex- PM_{10} , LSIndex and distance to sea. All the chosen spatial covariates were statistically significant at the 0.05 level with expected signs (Table 4). The average VIF for SO_2 , NO_2 and PM_{10} , were 1.24, 1.23 and 1.26, respectively, and the maximum VIF was 1.41. This demonstrated that there was a lack of significant collinearity between the chosen independent variables. The spatial autocorrelation for SO_2 , NO_2 and PM_{10} values was tested using GeoDa 0.9.5-i. A 4-nearest-neighbor approach in this study was used. Statistical significance was tested using a permutation test with 999 iterations. In this study, Moran's I values were -0.083 ($p = 0.057$), -0.092 ($p = 0.431$), and 0.013 ($p = 0.198$) for the SO_2 , NO_2 and PM_{10} model residuals, respectively. The R^2 values for PM_{10} , SO_2 and NO_2 were 0.84, 0.78 and 0.89, respectively, and RMSE values were 0.21, 0.32 and 0.18, respectively.

The 30 monitoring sites were divided into two parts. One part (22 monitoring sites) was used to establish multiple linear regression equations, and the other part (8 monitoring sites) was used for validation. The validation monitoring sites were selected randomly. Figure 6 compares the predicted SO_2 , NO_2 and PM_{10} concentrations to measured concentrations at 8 (out of 30) validation sites. Model predictions at validation monitoring sites went well, with predictions at validation sites generally within 15% of measured values.

Table 4 Multiple linear regression results for the association between dependent and independent variables

	β	t	p	VIF
Model for SO_2				
Intercept	0.063	8.473	0.006	1.12
PSIndex- SO_2 (10^{-5})	0.012	5.908	0.016	1.32
LSIndex	0.0009	4.864	0.017	1.21
Area of residential land (2 km)	0.008	2.745	0.021	1.34
Brightness	0.0005	4.765	0.015	1.19
Final LUR model including eight validation sites ($R^2 = 0.78$)				
Model for NO_2				
Intercept	0.042	9.760	0.000	1.05
PSIndex- NO_2 (10^{-5})	0.016	4.578	0.003	1.21
LSIndex	0.0008	7.456	0.018	1.33
Distance to expressway	-0.022	-2.807	0.019	1.24
Greenness	-0.0012	-3.957	0.014	1.32
Final LUR model including eight validation sites ($R^2 = 0.89$)				
Model for PM_{10}				
Intercept	0.112	8.453	0.002	1.08
Population density	0.014	5.612	0.016	1.32
PSIndex- PM_{10} (10^{-5})	0.019	4.628	0.025	1.41
LSIndex	0.0007	3.777	0.012	1.21
Distance to sea	-0.018	-6.705	0.007	1.27
Final LUR model including eight validation sites ($R^2 = 0.84$)				

β is the coefficient of independent variable. These are the t -statistics and their associated-tailed p -values used in testing whether a given coefficient is significantly different from zero. $\alpha = 0.05$. VIF: variance inflation factor.

2.5 Kriging of predicted SO_2 , NO_2 and PM_{10} concentrations

The origin was assigned to coordinates at latitude $38^\circ 32' 24'' \text{N}$ and longitude $116^\circ 42' 17'' \text{E}$, and 1×1 km grids were created over the whole study area. SO_2 , NO_2 and PM_{10} concentrations were calculated at each intersection using multiple linear regression equations. Maps of predicted annual average SO_2 , NO_2 and PM_{10} concentrations for the study area were interpolated based on the air pollutant concentrations at all the intersection points, and are shown in Fig. 7. The prediction maps were created using Kriging based on Arcgis 9.2.

There are three hotspots on the SO_2 concentration prediction map. One is located in the urban center, and the other two are located in the industrial area. The hotspot of the NO_2 concentration prediction map is located in the urban center. The hotspot of the PM_{10} concentration prediction map is close to the Bohai Sea.

3 Discussion

We incorporated data on industrial point sources to improve the model performance, and most point sources were included in this study. It should be acknowledged, however, that the dataset we used to identify point sources of pollution is likely to be incomplete. We also considered wind direction and the distance from each point source to the monitoring site, both of which may influence the extent and direction of the dispersion of pollution from these facilities.

To consider the impact of different sources, we calculated the PSIndex, LSIndex and area of different land use types (agricultural land, industrial land, commercial land, residential land, green space and water area) within

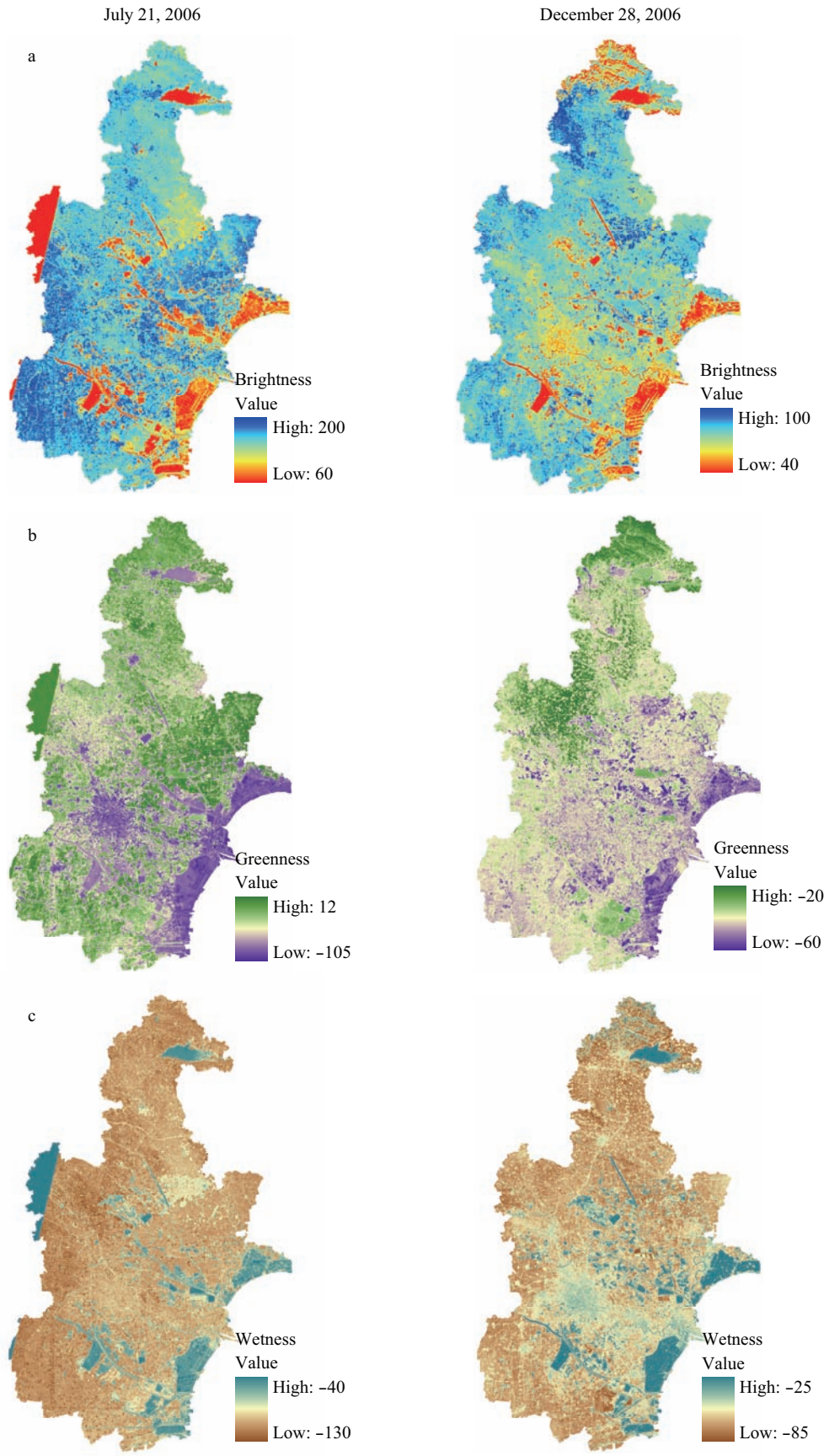


Fig. 5 Tasseled-cap brightness (a), greenness (b) and wetness (c).

different buffer radii (1 to 20 km). This method makes up for the lack of consideration of source impact based on the

LUR model. The LUR model was created using simple variables (such as length of roads within different buffer

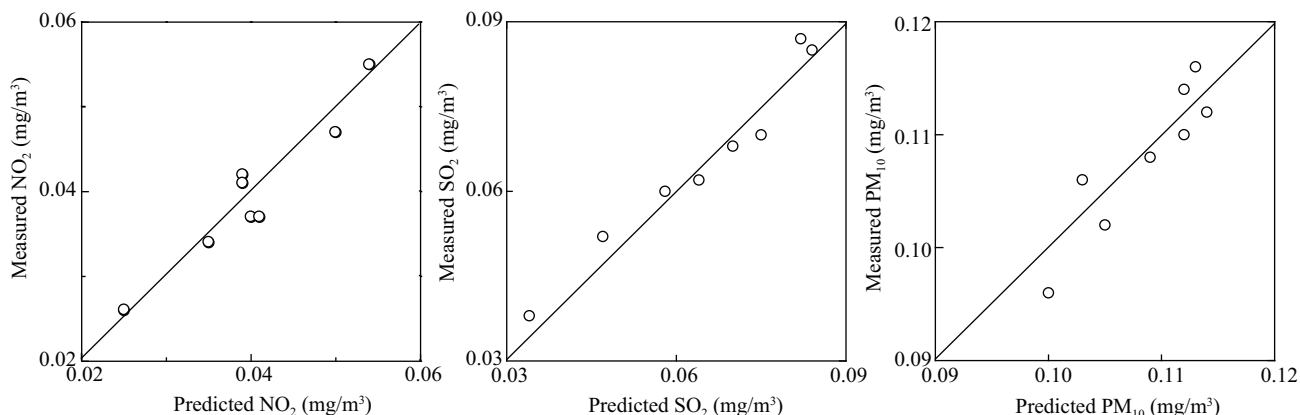


Fig. 6 Measured versus predicted concentration at validation monitoring sites.

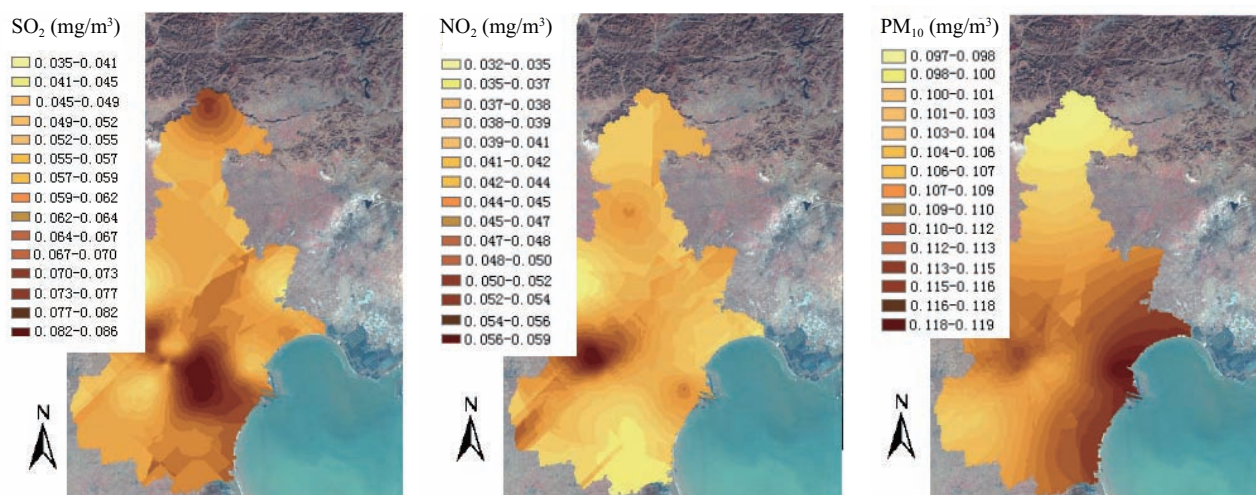


Fig. 7 Modeled SO₂, NO₂ and PM₁₀ concentrations prediction map using Kriging.

radii or wind frequency) and integrated variables (such as LSIndex), and the performance of the LUR model using integrated variables resulted in an increase in the R^2 values ranged 0.56–0.78, 0.76–0.89 and 0.64–0.84 for SO₂, NO₂ and PM₁₀, respectively. It is known that traffic variables and meteorological variables both affect the spatial distribution of the NO₂ concentration, while the relationship between traffic variables and the NO₂ concentration was not linear in this study. A linear relationship between the integrated variables and dependent variables was more consistent. This research demonstrated that SO₂, NO₂ and PM₁₀ could have high spatial extents of influence (the buffer radius of point sources was 15 km and the buffer radius of line sources was 5 km) and high background concentrations in the study area.

Compared to land use variables, the brightness, greenness and wetness from remote sensing data should more accurately characterize underlying surface conditions. In this study, brightness and greenness were found to be useful model inputs to improve the estimation of SO₂ and NO₂ concentrations. Brightness and greenness, as important variables for SO₂ and NO₂ in this study, were included in the LUR model as this resulted in 0.17 and 0.23 increases in the R^2 values.

Wheeler et al. (2008) applied the LUR model to predicting SO₂ concentration, and the R^2 was 0.69. The R^2

value of the LUR model for SO₂ was 0.78 in our study. Hoek et al. (2001) applied the LUR model to predicting the NO₂ concentration in the Netherlands, and the R^2 was 0.85. This was the highest R^2 for NO₂ in the previous studies, and the lowest R^2 of LUR models for NO₂ was 0.54. In our research, the R^2 of the LUR model for NO₂ was 0.89. Briggs et al. (2008) applied LUR to PM₁₀ in London, and the R^2 was 0.45–0.60. In our research, R^2 for PM₁₀ was 0.84. The performance of the LUR models for PM₁₀, SO₂ and NO₂ all improved compared to previous works.

The spatial distribution of the SO₂ concentration was relevant to industrial point sources, because the hotspot was located in the area including more point sources than other areas. The spatial distribution of the NO₂ concentration was centered in the downtown area, which had a denser traffic network and greater traffic volume. Based on the PM₁₀ concentration prediction map, marine aerosol may be a source of PM₁₀, because the hotspot was near to the sea.

The accuracy of the air pollutant concentration prediction map is key to the estimation of personal exposures. This study illustrated that enhanced LUR model selection and data input can produce much higher prediction powers when modeling air pollution in the city region. The accuracy increased when the LUR model was created using integrated variables and incorporating data on industrial

point sources in this study. This technique is readily applicable to epidemiology, exposure assessment and other similar studies.

Acknowledgments

This work was supported by the Special Environmental Research Funds for Public Welfare (No. 200909005), the National Natural Science Foundation of China (No. 20677030) and the Doctor Funds of Tianjin Normal University (No. 52XB1110). We thank the Tianjin Environmental Protection Bureau for help with air quality monitoring data; and the Tianjin Institute of Meteorological Science, for meteorological data.

References

- Araïn M A, Blair R, Finkelstein N, Brook J R, Sahsuvaroglu T, Beckerman B et al., 2007. The use of wind fields in a land use regression model to predict air pollution concentrations for health exposure studies. *Atmospheric Environment*, 41(16): 3453–3464.
- Brauer M, Hoek G, van Vliet P, Meliefste K, Fischer P, Gehring U et al., 2003. Estimating long-term average particulate air pollution concentrations: application of traffic indicators and geographic information systems. *Epidemiology*, 14(2): 228–239.
- Briggs D, 2005. The role of GIS: coping with space (and time) in air pollution exposure assessment. *Journal of Toxicology and Environmental Health, Part A* 68(13-14): 1243–1261.
- Briggs D, Collins S, Elliot P, Fischer P, Kingham S, Lebre E et al., 1997. Mapping urban air pollution using GIS: a regression-based approach. *International Journal of Geographical Information Science*, 11(7): 699–718.
- Briggs D J, de Hoogh C, Gulliver J, Wills J, Elliott P, Kingham S et al., 2000. A regression-based method for mapping traffic-related air pollution: application and testing in four contrasting urban environments. *Science of the Total Environment*, 253(1-3): 151–167.
- Briggs D, Hoogh C D, Gulliver J, 2008. Comparative assessment of GIS-based methods and metrics for modeling exposure to air pollution. *Journal of Toxicology and Environmental Health*, 67: 1223–1238.
- Crist E P, Cicone R C, 1984. A physically-based transformation of thematic mapper data – the TM tasseled cap. *IEEE Transactions on Geoscience and Remote Sensing*, GE-22(3): 256–263.
- Gilbert N L, Goldberg M S, Beckerman B, Brook J R, Jerrett M, 2005. Assessing spatial variability of ambient nitrogen dioxide in Montreal, Canada, with a land-use regression model. *Journal of the Air & Waste Management Association*, 55(9): 1059–1063.
- Henderson S B, Beckerman B, Jerrett M, Brauer M, 2007. Application of land use regression to estimate long-term concentrations of traffic-related nitrogen oxides and fine particulate matter. *Environmental Science and Technology*, 41(7): 2422–2428.
- Hoek G, Meliefste K, Brauer M, Vliet P V, Brunekreef B, Fischer I et al., 2001b. Risk assessment of exposure to traffic-related air pollution for the development of inhalant allergy, asthma and other chronic respiratory conditions in children (TRAPCA). Final Report, IRAS. University Utrecht, Utrecht.
- Hoek G, Beelen R, Hoogh K D, Vienneau D, Gulliver J, Fischer P et al., 2008. A review of land-use regression models to assess spatial variation of outdoor air pollution. *Atmospheric Environment*, 42(33): 1–18.
- Jerrett S, Arain A, Kanaroglou P, Beckerman B, Potoglou D, Sahsuvaroglu T et al., 2005. A review and evaluation of intraurban air pollution exposure models. *Journal of Exposure Science and Environmental Epidemiology*, 15(2): 185–204.
- Kashima S, Yarifuji T, Tsuda T, Doi H, 2009. Application of land use regression to regulatory air quality data in Japan. *Science of the Total Environment*, 407(8): 3055–3062.
- Mavko M E, Tang B, George L A, 2008. A sub-neighborhood scale land use regression model for predicting NO₂. *Science of the Total Environment*, 398(1-3): 68–75.
- Mukerjee S, Smith L A, Johnson M M, Neas L M, Stallings C, 2009. Spatial analysis and land use regression of VOCs and NO₂ from school-based urban air monitoring in Detroit/Dearborn, USA. *Science of the Total Environment*, 407(16): 4642–4651.
- Ross Z, Jerrett M, Ito K, Tempalski B, Thurston G D, 2007. A land use regression for predicting fine particulate matter concentrations in the New York City region. *Atmospheric Environment*, 41(11): 2255–2268.
- Ryan P H, LeMasters G K, Levin L, Burkle J, Biswas P, Hu S et al., 2008. A land-use regression model for estimating microenvironmental diesel exposure given multiple addresses from birth through childhood. *Science of the Total Environment*, 404(1): 139–147.
- Slama R, Morgenstern V, Cyrys J, Zutavern A, Herbarth O, Wichmann H E et al., 2007. Traffic-related atmospheric pollutants levels during pregnancy and offspring's term birth weight: a study relying on a land-use regression exposure model. *Environmental Health Perspectives*, 115(9): 1283–1292.
- Su J G, Brauer M, Ainslie B, Steyn D, Larson T, Buzzelli M, 2007. An innovative land use regression model incorporating meteorology for exposure analysis. *Science of the Total Environment*, 390(2-3): 520–529.
- Tianjin Bureau of Environmental Protection, 2007. Tianjin environmental quality reports (2006). Tianjin Environmental Monitoring Center, Tianjin.
- Wheeler A J, Smith-Doiron M, Xu X, Gilbert N L, Brook J R, 2008. Intra-urban variability of air pollution in Windsor, Ontario measurement and modeling for human exposure assessment. *Environmental Research*, 106(1): 7–16.

JOURNAL OF ENVIRONMENTAL SCIENCES

Editors-in-chief

Hongxiao Tang

Associate Editors-in-chief

Nigel Bell Jiuhui Qu Shu Tao Po-Keung Wong Yahui Zhuang

Editorial board

R. M. Atlas University of Louisville USA	Alan Baker The University of Melbourne Australia	Nigel Bell Imperial College London United Kingdom	Tongbin Chen Chinese Academy of Sciences China
Maohong Fan University of Wyoming Wyoming, USA	Jingyun Fang Peking University China	Lam Kin-Che The Chinese University of Hong Kong, China	Pinjing He Tongji University China
Chihpin Huang "National" Chiao Tung University Taiwan, China	Jan Japenga Alterra Green World Research The Netherlands	David Jenkins University of California Berkeley USA	Guibin Jiang Chinese Academy of Sciences China
K. W. Kim Gwangju Institute of Science and Technology, Korea	Clark C. K. Liu University of Hawaii USA	Anton Moser Technical University Graz Austria	Alex L. Murray University of York Canada
Yi Qian Tsinghua University China	Jiuhui Qu Chinese Academy of Sciences China	Sheikh Raisuddin Hamdard University India	Ian Singleton University of Newcastle upon Tyne United Kingdom
Hongxiao Tang Chinese Academy of Sciences China	Shu Tao Peking University China	Yasutake Teraoka Kyushu University Japan	Chunxia Wang Chinese Academy of Sciences China
Rusong Wang Chinese Academy of Sciences China	Xuejun Wang Peking University China	Brian A. Whitton University of Durham United Kingdom	Po-Keung Wong The Chinese University of Hong Kong, China
Min Yang Chinese Academy of Sciences China	Zhifeng Yang Beijing Normal University China	Hanqing Yu University of Science and Technology of China	Zhongtang Yu Ohio State University USA
Yongping Zeng Chinese Academy of Sciences China	Qixing Zhou Chinese Academy of Sciences China	Lizhong Zhu Zhejiang University China	Yahui Zhuang Chinese Academy of Sciences China

Editorial office

Qingcai Feng (Executive Editor) Zixuan Wang (Editor) Suqin Liu (Editor) Zhengang Mao (Editor)
Christine J Watts (English Editor)

Journal of Environmental Sciences (Established in 1989)

Vol. 24 No. 7 2012

Supervised by	Chinese Academy of Sciences	Published by	Science Press, Beijing, China
Sponsored by	Research Center for Eco-Environmental Sciences, Chinese Academy of Sciences	Distributed by	Elsevier Limited, The Netherlands
Edited by	Editorial Office of Journal of Environmental Sciences (JES) P. O. Box 2871, Beijing 100085, China Tel: 86-10-62920553; http://www.jesc.ac.cn E-mail: jesc@263.net , jesc@rcees.ac.cn	Domestic	Science Press, 16 Donghuangchenggen North Street, Beijing 100717, China Local Post Offices through China
Editor-in-chief	Hongxiao Tang	Foreign	Elsevier Limited http://www.elsevier.com/locate/jes
CN 11-2629/X	Domestic postcode: 2-580	Printed by	Beijing Beilin Printing House, 100083, China
		Domestic price per issue	RMB ¥ 110.00

ISSN 1001-0742

